Smart Geotechnics for Smart Societies – Zhussupbekov, Sarsembayeva & Kaliakin (Eds)

Influence of microscale cohesive contacts on the macro-behaviour of soils through DEM investigation

T. Doan
PhD Candidate, Transport Research Centre, Faculty of Engineering & Information Technology, University of Technology Sydney, New South Wales, Australia

B. Indraratna
Distinguished Professor, Transport Research Centre, Faculty of Engineering & Information Technology, University of Technology Sydney, New South Wales, Australia

T.T. Nguyen
Research Fellow, Transport Research Centre, Faculty of Engineering & Information Technology, University of Technology Sydney, New South Wales, Australia

C. Rujikiatkamjorn
Professor, Transport Research Centre, Faculty of Engineering & Information Technology, University of Technology Sydney, New South Wales, Australia

ABSTRACT: Microscale contacts are inherent in most geotechnical failures such as soil liquefaction, landslides and internal instability, thus study of these failures based on microscale concepts can significantly enhance our intrinsic understanding as well as the quality of prediction and designs. Despite rapidly increasing investigation on micro-mechanisms of soil failures, especially based on Discrete Element Method (DEM), cohesive behaviours of particles are usually ignored and simplified, resulting in incomplete and/or inaccurate understanding. My study aims to overcome this imperative limitation and improve our modelling capability by investigating the influence of microscale cohesive contacts on fundamental soil behaviours such as the formation of angle of repose and direct shear. Different degrees of cohesion between particles are incorporated into DEM models and the results are validated against experimental data. The results show cohesive contacts can significantly affect soil behaviour and the predicted outcomes if they are not considered properly. The prediction capability of this DEM model can be further applied to study the cohesive behaviour of geomaterials in various geotechnical problems such as soil clogging and debris flow.

1 INTRODUCTION

Soils are naturally occurring materials composed of constituent grains of varying sizes, shapes and compositions that are in contact with each other. The particulate nature of soils gives rise to complex interactions between particles such as friction and inter-particle cohesion and these particle-scale contacts play a crucial role in determining the overall behaviour of the soil including its strength, stiffness, and deformation characteristics. To understand the macro-response of soils, it is imperative to take their particulate nature and micro-scale contacts into account, and this requires the use of advanced approaches such as the discrete element method (DEM) to capture the particle-scale response. Previous studies have successfully employed DEM techniques to capture a range of complex soil responses; for instance, non-linear stress and strain responses (O'Sullivan, 2011), stress-state dependency (Lommen et al., 2014), critical-state behaviour (Phan et al., 2021), internal instability (Nguyen and Indraratna, 2020a), and many others. However, most previous studies have mainly considered cohesionless frictional materials

DOI: 10.1201/9781003299127-20

whereas cohesive contacts are ignored leading to inaccurate or incomplete analysis. This means increasing effort is needed to simulate the cohesive behaviour of soils more accurately in DEM.

The cohesive behaviour of soils, which refers to the bonding and inter-particle cohesion between soil particles, plays a crucial role in the stability of soils and their resistance to macro-scale failures such as liquefaction, landslides and slope instability (Mitchell and Soga, 2005). At the macro-scale, the classical Mohr-Coulomb theory states that the cohesive strength of soils contributes to the overall shear strength, providing resistance to sliding and shear deformation. At the microscopic level, the cohesive strength is characterised by the presence of cohesive contacts between soil particles, which mainly include van der Waal forces between fine particles (Parteli et al., 2014), electrostatic forces (Endres et al., 2021) and capillary interactions between wet particles (Wang et al., 2018). As these cohesive forces can occur individually or concurrently, the effort to consider these non-linear forces in DEM contacts can be complex and computationally intensive. In addition, measuring the micro-scale cohesive forces between individual particles in laboratory testing is arduous, which makes it more difficult to obtain accurate and reliable data to support the modelling of this behaviour. Moreover, cohesion is often dependent on several factors such as moisture contents and types of soil, making it problematic to develop a comprehensive model to accurately represent this behaviour. In a nutshell, the cohesive behaviour of soils, despite its significant influence on the performance of soils, is often ignored in DEM simulations due to difficulties in modelling and characterising this ambiguous behaviour.

To overcome limitations regarding the computational cost, it is common to use some of the well-established physics models such as the JKR (Johnson-Kendall-Roberts) and the DMT (Darjaguin-Muller-Toporov) to describe the attraction forces between two contacting particles. While JKR theory is developed to capture the short-range, strong surface forces between large and deformable bodies, DMT regime corresponds to an opposite type of materials (i.e., hard, small radius, and long-range attraction forces). Previous studies stated that cohesive forces calculated by the JKR model are closely approximated with experimental measurements by AFM for various materials (Jones, 2003). Therefore, the JKR model has been increasingly used to model fine and wet materials in which cohesive interactions dominate the macroscopic behaviour of materials considerably (Deng and Davé, 2013, Hassanzadeh et al., 2020). In this study, the JKR theory will be incorporated into the DEM contact mechanics to capture the cohesive behaviour of geomaterials.

This study aims to apply DEM model which simultaneously considers frictional (sliding) contact, rolling resistance and micro-scale cohesive forces, with a special emphasis on the modelling the cohesive behaviour of geomaterials. It will also provide a thorough investigation into the micro-cohesive effects on macro-behaviour of soils while flowing and shearing. The application of the current cohesive model is validated against experimental tests such as the angle of repose (AoR) and direct shear tests (DST). Furthermore, extensive analysis is conducted to investigate the effect of cohesive contact forces on the macro- and micro-response of soils. Based on this analysis, a linkage between micro-scale parameter and macro-scale property can be provided to obtain a better understanding of the overall soil responses.

2 DEM COHESIVE MODEL AND NUMERICAL ANALYSIS

2.1 *DEM cohesive model*

For granular materials, the Hertz-Mindlin contact model has been successfully adopted by previous studies (Zhu et al., 2007) to compute the normal and tangential contact forces in relation to elastic deformation between particles, therefore, this model will be employed in the current study. In the Hertz-Mindlin model, the respective contact forces are determined from contact stiffnesses as follows:

$$k_n = \frac{4}{3} E^* \sqrt{R^* \delta_n} \tag{1}$$

$$k_t = 8G^* \sqrt{R^* \delta_n} \tag{2}$$

where E^*,G^* and R^* are the effective Young's modulus, shear modulus, and radius of two particles respectively, and δ_n is the normal overlap or displacement. Further information to determine these input parameters is provided elsewhere (Li et al., 2005, Zhu et al., 2007).

Following most of DEM studies in the literature, spheres are commonly used owing to the modelling simplicity and contact detection efficiency. However, this simplification leads to the loss of shape effects (i.e., angularity and interlocking) and results in discrepancies between numerical and physical results. Hence, to compensate for realistic shapes in DEM, a concept of using rolling resistance model has been developed by several researchers (Ai et al., 2011) to account for a rolling resistance torque opposing the free-rolling tendency of spheres. In this study, a rolling resistance model known as elastic-plastic spring-dashpot model (EPSD2) will be used as this model has been recognised to prevent oscillatory behaviour and provide quasi-static simulations. The rotational resistance torque is a function of a rolling friction coefficient μ_r as follows:

$$\left| M_{ij}^r \right| \leq \mu_r R^* \left| F_{ij}^n \right| \tag{3}$$

For the cohesive behaviour, the cohesive model proposed by Doan et al. (2023) was used to couple the simplified Hertz-Mindlin contact mechanics and JKR theory to capture the elasto-cohesive response between particle contacts. The fundamental concept of JKR theory characterises the attractive forces between solids by an additional tensile stress at the contact boundary leading to a finite contact area even at zero load, as shown in Figure 1.

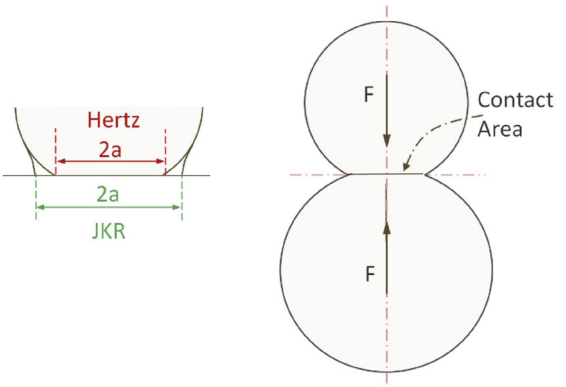

Figure 1. Schematic of the force-displacement relationship in JKR theory (refer to (Roessler and Katterfeld, 2019)).

The JKR theory used a concept of energy balance method to determine the surface attraction forces (i.e., vdW forces) based on their respective surface energies. The application of JKR has been expanding across multi-disciplinary fields to model the cohesive behaviour of powders, micro-scale particles and geomaterials (Deng and Davé, 2013, Barthel, 2008). The contact forces, deformation and radius are derived by JKR theory as follows:

$$\boldsymbol{F_{ij}^{JKR}} = \frac{4E^* a^3}{3R^*} - \sqrt{8\pi E^* \gamma_E a^3} \tag{4}$$

$$\delta_{ij}^{JKR} = \frac{a^2}{R^*} - \sqrt{\frac{2\pi a \gamma_E}{E^*}} \tag{5}$$

$$a = \frac{3R^*}{4E^*}\left[\boldsymbol{F_{ij}^{JKR}} + 3\pi\gamma_E R^* + \sqrt{\boldsymbol{F_{ij}^{JKR}} 6\pi\gamma_E R^* + (3\pi\gamma_E R^*)^2}\right] \tag{6}$$

Where as F_{ij}^{JKR} and δ_{ij}^{JKR} are the cohesive contact force and deformation according to JKR formulations; γ_E is an effective surface energy between two particles and a is the contact radius. As the computation of the contact radius a is prohibitively demanding and not easily obtained, the original JKR model is subjected to some simplifications leading to the development of the simplified JKR model (SJKR). Instead of using the surface energies, the SJKR model employs an empirical and numerical cohesive term named Cohesion Energy Density (CED), which is defined as the volumetric energy needed to separate the attractive interactions between two particles. In this SJKR model, the cohesive force is computed as a function of CED (J/m^3) and the contacting area A as follows:

$$\boldsymbol{F_{ij}^{JKR}} = CED \times A \tag{7}$$

As described by Doan et al. (2023), the term CED can be related to the surface energy which is a physical property and can be theoretically measured for any materials, as follows:

$$CED = \sqrt[3]{\frac{8E^{*2}\gamma_E}{3R^*\pi^2}} \tag{8}$$

2.2 *Numerical validation with experimental tests studying the flowing behaviour of soil (Angle of repose test)*

Prior to further developments, it is crucial to test the proposed DEM model with micro-scale cohesive forces against fundamental tests such as the angle of repose (AoR) test. The angle of repose is defined in Terzaghi (1943) as the steepest slope of angle that a soil can form without external effects such as confining pressures. The AoR test is demonstrated by numerous studies (Li et al., 2005, Derakhshani et al., 2015) to provide valuable information about the interparticle forces and friction angle of materials, both of which are critical for geotechnical designs and analysis. Previous studies have shown that the AoR is highly sensitive with the presence of cohesive forces, hence, a neglect of cohesive contacts results in an underprediction of the AoR value. Therefore, incorporating the cohesive forces in DEM contact mechanics is prominent to capture the macro-response of materials more realistically.

To simulate the AoR test, a lifting cylinder test was chosen due to its simplicity to determine the AoR of geomaterials. Sandy soils in dry and wet states were selected to study the cohesionless and cohesive behaviour of materials in the AoR test. For wet sands, the inter-particle cohesive forces mainly take on a form of liquid-bridging forces which result in the generation of capillary and viscous forces. The SJKR model was used to represent the capillary forces, while the influence of viscous force was deemed insignificant in quasi-static conditions. To simulate the AoR test in DEM, several input parameters which have been consistently provided in previous studies were collated in the Table 1 below. Additionally, as the rolling friction coefficient and micro-scale cohesive forces (i.e., calculated from the Cohesion Energy Density (CED) value) are different among materials, these values will be calibrated to match with the current experimental data. For the calibration of rolling resistance coefficient, this value varies greatly in the literature ranging from 0.1 (i.e., highly spherical particles) to 0.5 (i.e., highly angular shape), hence, this range was used in the current study. The calibration of CED parameter was based on past studies which reasonably captured the cohesive effect of various materials. In the current investigation, CED values were selected from 0 for the cohesionless state to 5 x 10^5 (J/m^3) for the cohesive state. The variations of rolling resistance coefficients and CED were summarised in Table 2.

To verify that the DEM simulations are valid, the numerical results were compared with the experimental tests conducted on wet sands from Roessler and Katterfeld (2019). It is worthy to

Table 1. The input parameters for the current DEM study.

Parameters	Inputs	References
Particle density (kg/m^3)	2650	
Poisson's ratio	0.3	
Shear modulus (Pa)	10x10^7	
Restitution coefficient	0.2	(Behjani et al., 2017)
Particle-wall friction coefficient	0.36	(Roessler and Katterfeld, 2019)
Particle-particle sliding friction	0.5	(Nguyen and Indraratna, 2020a, Phan et al., 2021)
Timestep (s)	10^{-5}	10% Rayleigh time step
Gravitational acceleration (m/s^2)	9.81	

Table 2. The calibrated parameters in DEM.

Parameters	Value range	Value increment
Rolling friction coefficient (μ_r)	0.1 - 0.5	0.1
Cohesion Energy Density (CED) (J/m^3)	0 - 5x10^5	1x10^5

note that instead of comparing the angle of repose (AoR) values which can be highly variable and not appropriate for the characterisation of cohesive materials, the flowability of materials was selected for comparison. The flowability of wet soils was observed to be dependent on a lifting height (h) which was defined as a gap between the bottom of the cylinder and the horizontal base, hence, the flow response of soils was captured in four separate stages (i.e., h = 90 mm, 120 mm, 160 mm and 280 mm for a 375mm-high cylinder). Figure 2 demonstrates that DEM simulations can mimic the flow characteristics of materials in the experiments very well. More specifically, at the initial stage of the tests when the lifting height remains small (h = 90 mm), a solid column of materials is witnessed in both DEM and experiments without any bending or spreading of materials yet as the cohesive and frictional forces are sufficient to counteract with the self-weight of the material. This phenomenon is repeatedly observed in the physical tests by Roessler and Katterfeld (2019). Then, when the gap is increased further, the column of materials starts to collapse, leading to the further spreading of materials to form a convex slope as seen in Stage 2, 3 in Figure 2. Finally, at stage 4 when the cylinder is sufficiently lifted, a quasi-static heap of wet sand materials is formed physically and numerically. To sum up, the DEM simulations incorporating cohesive forces were in good agreement with the experimental results. For a further development, the DEM model can be improved to simulate cracks appearing in the heaps of wet sands owing to difficulties to maintain a uniform and homogenous distribution of moisture content in the experiment.

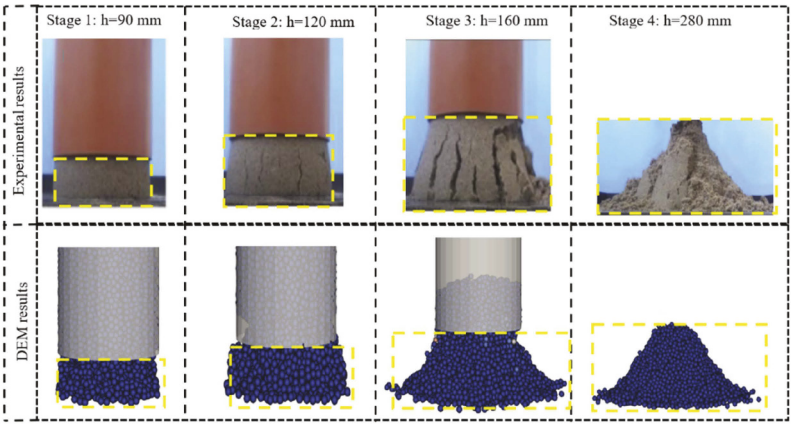

Figure 2. Comparison between DEM models and experimental tests.

The experimental tests from Roessler and Katterfeld (2019) also found out that the bending of the column of materials at different phases was reproducible and can be quantified, hence, this criteria was chosen for a quantitative comparison between DEM and experiments. The bending of material was characterised by a parameter named the relative pile diameters (d_{rel}) to compare between the diameter of the pile d_{pile} and the diameter of the cylinder ($d_{cylinder}$) (i.e., the formulation was given in Doan et al. (2023)). Figure 3 indicates that with a small lifting height h = 80 mm, the pile remains nearly vertical with 2.3 % bending in DEM results and 2.1 % bending in experiments. However, when the cylinder is lifted further, the slope of materials curves more significantly with 25.1 % of convex bending in DEM and 25% in the referenced case. By comparing the DEM results and experiments both qualitatively and quantitatively, DEM simulations represented experimental observations very well. More particularly, the DEM results also captured many important features of the cohesive behaviour of soils; for example, when cohesive forces were present, the flowability of materials was significantly hindered as compared to the free-flowing feature of cohesionless materials.

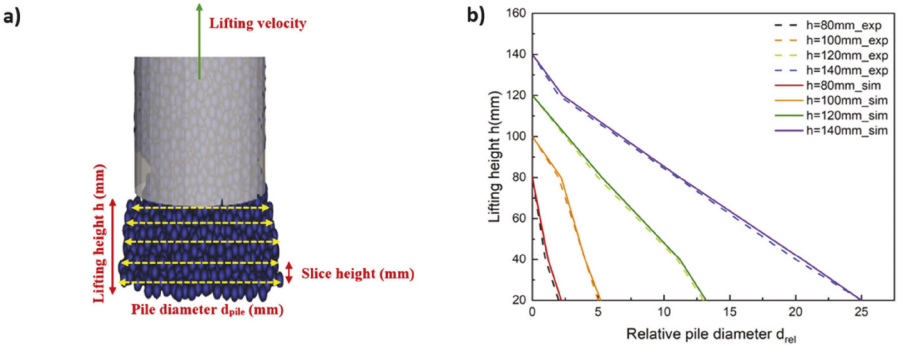

Figure 3. Quantitative comparison of the convex bending between DEM and experimental results from Roessler and Katterfeld (2019) (modified after (Doan et al., 2023)).

2.3 *Numerical calibration and comparison with experimental test for loading condition in Direct Shear Test (DST)*

After the DEM cohesive model was validated against the fundamental angle of repose test, more efforts are needed to test the capability of the cohesive model under external loading. It is critical to study the behaviour of a soil under loading conditions such as the shear strength and deformation of soil in several contexts, namely, the soil bearing capacity and settlement characteristics, the stability of slopes and retaining walls, and soil liquefaction and erosion. This study aims to investigate the underlying mechanics of the cohesive effects on the shear behaviour of soils via the use of the proposed DEM cohesive model and standardised Direct Shear Tests (DST). A validation of the current DEM model is performed by using a series of physical direct shear test to compare with the equivalent numerical results.

A series of direct shear tests were conducted using DEM simulations to capture the effect of microscopic cohesion on the shear strength of cohesive materials. The simulations were carried on a realistic grading of geomaterials with a similar particle size distribution as in the experiment as shown in . The schematic of the direct shear test (DST) is given in Figure 5.

To fill in a numerical shear box as shown in Figure 5, the number of particles was nearly 100,000 particles which by far surpassed the minimum number of 30,000-50,000 particles required for the friction angle and the dilation angle to be captured well in DEM results (Ni et al., 2000). In addition, the ratio between the length of the shear box and the maximum particle size was nearly 50 times, which exceeded the ratio of 10 times empirically defined in ASTM standards to minimize the boundary effects. Besides particle sizes, other microparameters such as the Young's Modulus, Poisson's ratio in DEM simulations were selected based on previous studies (refers to Table 3).

For comparison with experimental results, soils in cohesionless and cohesive states were used to compare with DEM results. For the dry sand without cohesion, the shear strength is primarily controlled by the sliding and rolling friction between two particles. These particle-level parameters are difficult to measure, hence they are often calibrated in numerical procedure. This study varied sliding and rolling friction to match the experimental results with experimental data. As shown in Figure 6, both experimental and numerical results exhibit a strain softening behaviour, where the shear stresses reach a peak value and then gradually decrease. A dimensionless parameter called stress ratio is used to normalise the shear stresses with the applied normal stresses. The maximum stress ratios in DEM simulations for three levels of normal stresses (i.e., 45 kPa, 90 kPa, and 133 kPa) are very close with the experimental values, confirming the accuracy of the strength parameters predicted in DEM simulations. In addition, comparison between dilative behaviour between DEM and experiments indicates a reasonable agreement confirming the predictability of DEM both in terms of strength and deformation of the cohesionless soil.

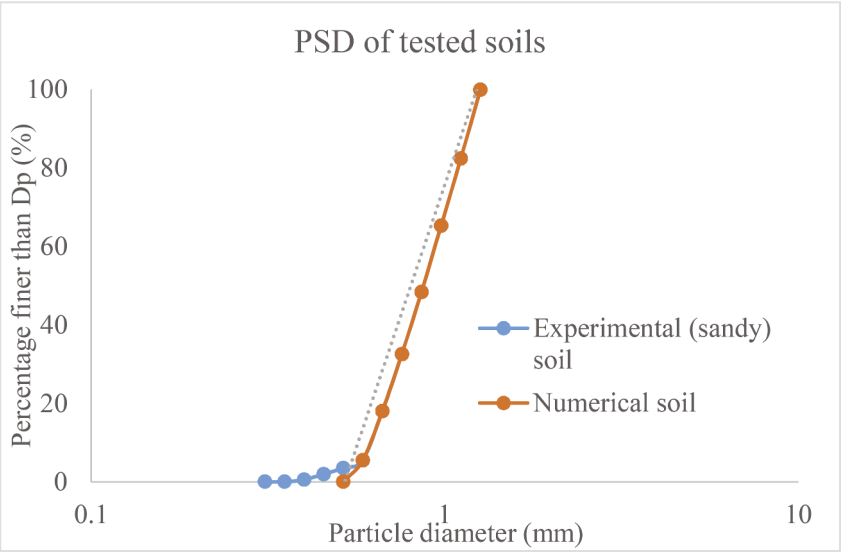

Figure 4. PSD used in DEM and experiments for the direct shear tests.

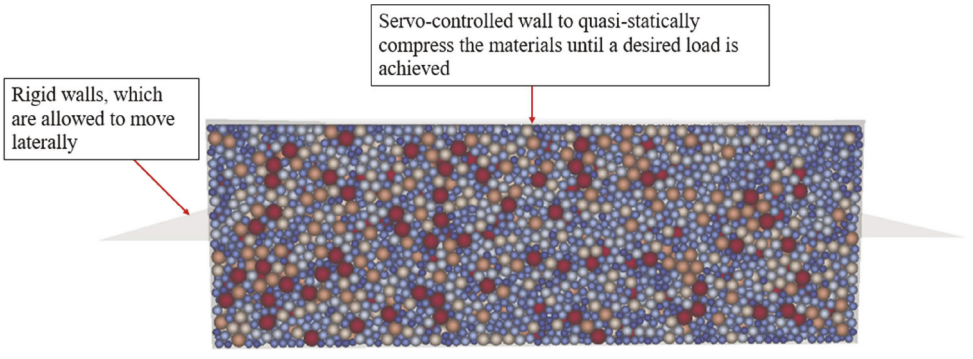

Figure 5. Direct shear test simulated in DEM.

For the cohesive state of materials, the sandy samples were mixed with a certain degree of water (i.e., moisture content 10%) to generate weakly cohesive forces arising

mainly from capillary interactions. Figure 7 demonstrates the stress-strain curves in the experiments with 10 % water content and DEM model introducing cohesive forces from CED value (i.e., CED = 4 x 10^5 J/m^3). Results from DEM simulations show a similar trend as those of the experimental observations. In general, DEM model has successfully captured the main features of the experimental outcomes, such as the peak strength and the softening response under various cohesion levels (i.e., cohesionless and weakly cohesive state).

Table 3. DEM input parameters for the direct shear simulations.

Parameters	Inputs	References
Particle density (kg/m^3)	2650	(Nguyen and Indraratna, 2020b)
Poisson's ratio	0.3	
Shear modulus (Pa)	10x10^7	
Restitution coefficient	0.7	
Particle-wall friction coefficient	0.1	(Cui and O'Sullivan, 2006)
Timestep (s)	10^{-7}	10% Rayleigh time step
Gravitational acceleration (m/s^2)	9.81	

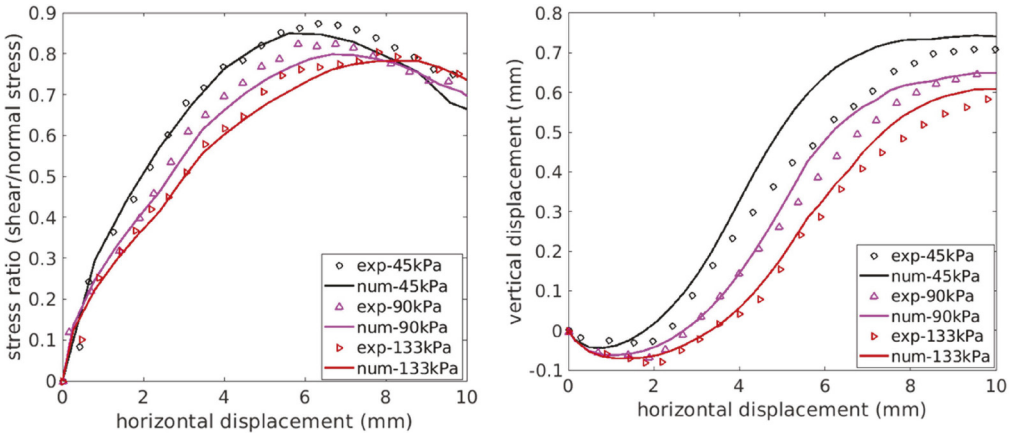

Figure 6. Comparison between DEM and experiments for the referenced cohesionless material.

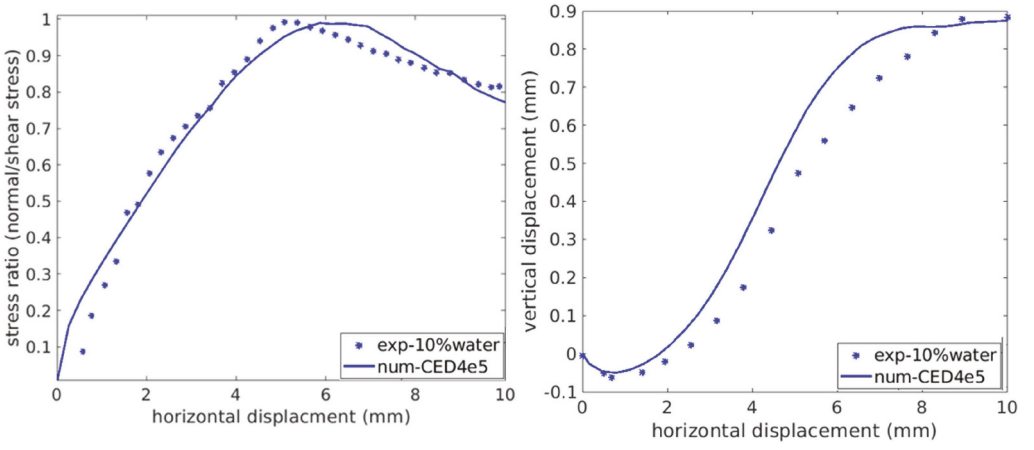

Figure 7. Comparison between the shear behaviours of materials in experiments and DEM under cohesion levels and normal stress of 45 kPa.

3 RESULTS AND DISCUSSION

After completing the calibration process where the DEM results were reasonably validated against fundamental experiment tests such as the Angle of Repose (AoR), and the Direct Shear Test (DST), this section will discuss some of the insights obtained from DEM analysis to demonstrate the effect of micro-scale cohesion on the macro- and micro-responses of soils.

3.1 *The cohesive effect on the macro-response in AoR test*

Figure 8 shows a three-dimensional plot indicating an interactive role between micro-scale friction and cohesion on the angle of repose. It shows that with increasing cohesion levels (from 0 to $5x10^5$ J/m^3), AoR values increase proportionally regardless of the rolling friction value. More importantly, without the effect of cohesion, the AoR is only able to increase up to 31°, however, with the presence of CED values, the AoR values can reach a higher value ranging from 40° to 45°. This finding is supported by experimental observations presented in (Mason et al., 1999, Mitarai and Nori, 2006) implying that the angle of repose of partially saturated materials is generally higher than a cohesionless dry system, nonetheless, these studies did not study how various cohesion levels (i.e., moisture content) affect the forming of this angle. This study also discovers that the numerical AoR values can increase up to 45°, which falls within the range of AoR values for cohesive materials (Beakawi Al-Hashemi and Baghabra Al-Amoudi, 2018). The reason for this rising AoR can be linked to the effect of cohesive forces on the flowing behaviour of soils as with the cohesive presence, the additional tensile forces prevent the separation between particles and consequently, hinder the flowing capacity of the materials.

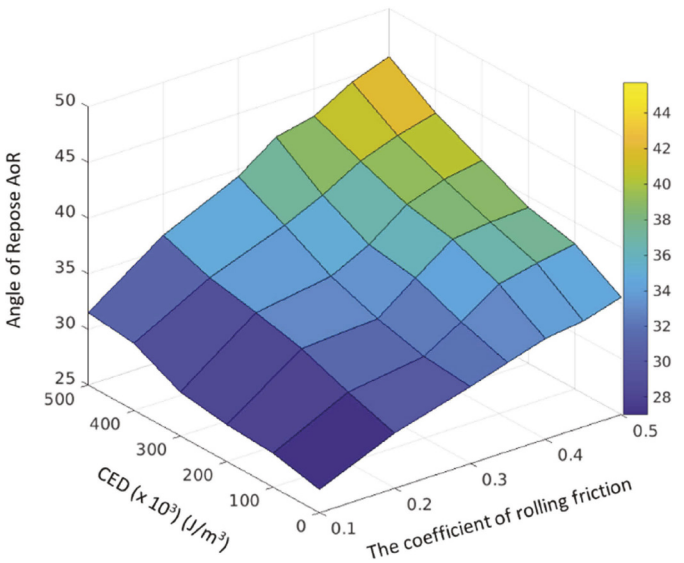

Figure 8. The effect of micro-scale cohesive forces (determined from CED values) on AoR value.

Besides AoR values, the overall porosity is a significant consideration to reflect the microstructure and the compactness of the pile, which is also dependent of micro-scale parameters such as inter-particle cohesion and friction. To compute the porosity value, this study developed a Python program incorporating Monte-Carlo algorithm to approximate the void fraction (i.e., or porosity) within a specific volume of materials. Figure 9 shows the changes of porosity with cohesion and rolling friction levels as when the cohesive and frictional forces increase, the porosity increases as well. For instance, with a given value of rolling friction (for example, 0.1), the porosity value increases from 0.586 to 0.6 when cohesion value CED

increases from 0 to $5x10^5$ (J/m^3). This tendency is due to a fact that when cohesive forces are present, the micro-structure of materials is seen gradually separated with large voids and chain-connected connections (Rognon et al., 2007, Xu et al., 2007). The increased porosity with cohesion content has been observed experimentally by (Gratchev et al., 2006, Goudarzy et al., 2021), indicating that when cohesive fines are present, the structures become separated with open micro-fabrics.

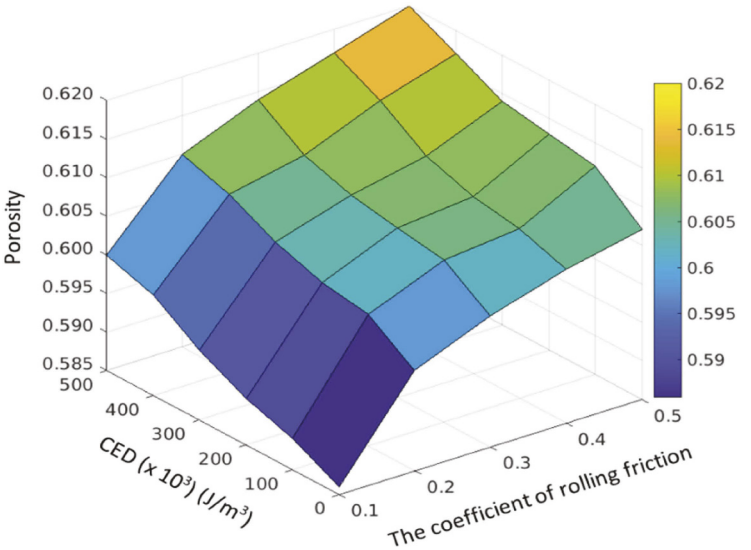

Figure 9. The cohesive effect on the porous structure of the AoR pile.

3.2 *Effect of cohesive contact on the micro-mechanical response of AoR via the analysis of coordination number*

The coordination number CN (i.e., refers to the number of neighbours per particle) is determined with respect to the total number of contacts (n_c) and number of particles (n_p) as follows:

$$CN = \frac{2n_c}{n_p} \tag{9}$$

Figure 10 demonstrates that the coordination number, which is with the spatial arrangement of the particles, was negatively dependent on the values of cohesion and rolling friction coefficients. In the case of cohesive materials as CN values decrease with increasingly cohesive particles (i.e., CED increased from 0 to 5 x 10^5). The similar tendency is also observed in the case of cohesionless material (CED = 0), the CN value experiences a reduction from 8 to 7.3 when the particles become more rotationally resistant. When the values of cohesion and rolling friction are both high, the CN value continuously reduces to reach a small value between 6 and 7. This means when cohesive forces or frictional forces dominate, the system becomes less densified with fewer contacts per particles.

To gain insights into how the cohesive and rolling resistant forces impact the coordination number, the balance of all external and internal forces acting on particles is analysed. According to Yu et al. (2003), cohesionless granules commonly have an average of six contacts per particle to counterbalance the gravitational forces. However, when both cohesion and rolling friction increase, the coupled effect of cohesive and frictional forces is sufficient to resist the driving force of gravity, allowing stability to be achieved with fewer particle-to-particle contacts, as few as two per particle, as demonstrated by Xu et al. (2007).

3.3 *Particle-scale insights into the movement of individual particles in the AoR test*

This study also attempts to track the kinetic energy and the total displacement of particles which have not been provided in previous studies and explores how cohesive forces affect the materials at the particle-scale level. Figure 11a compares the kinetic energy between the cohesionless and cohesive systems and reveals that the with cohesive forces, the KE of the system reaches a smaller peak. In addition, the cohesionless samples peak and stabilise at an earlier stage than the cohesive

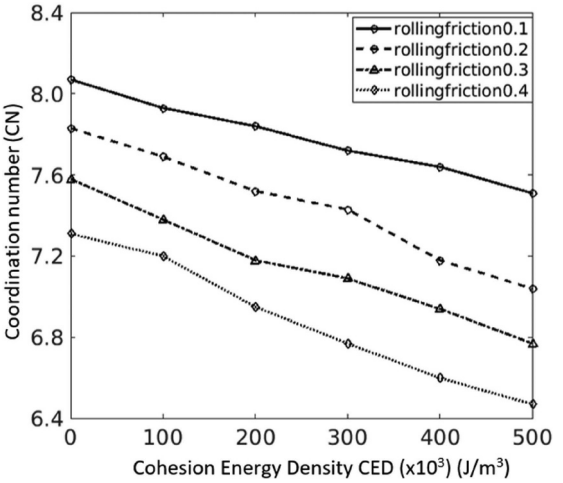

Figure 10. The cohesive influence on the internal fabric of AoR test.

samples, indicating that more time is required for the cohesion-induced materials to dissipate the kinetic energy. This is because as the level of cohesion increases, the interparticle forces become stronger and the particles tend to move together as agglomerates instead of as individual units. As a result, cohesive particles exhibit a more gradual and less brittle response, with a delay in the initiation and dissipation of kinetic energy compared to non-cohesive particles. This is shown in the Figure 11a that the non-cohesive materials take about 17s to reach a stable state, while the cohesive materials need more than 19s to stabilise. Moreover, Figure 11b captures the total displacement of particles with and without cohesion in the forming of the angle of repose AoR. The

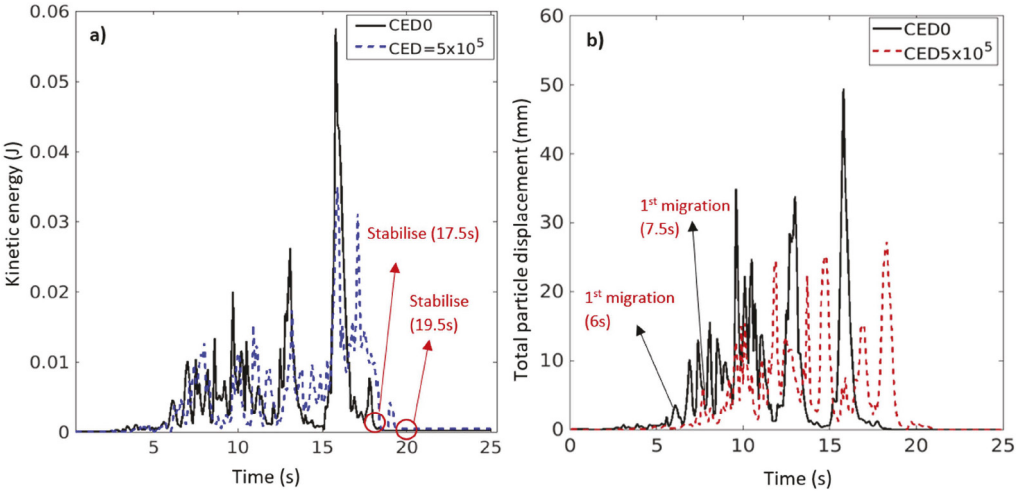

Figure 11. Particle-scale analysis in the AoR test in terms of a) kinetic energy KE and b) particle displacements.

cohesionless particles (i.e., black solid line) experience a much higher displacement (i.e, around 49 mm) than the displacement that the cohesive materials can make (i.e., 35 m). In addition, similar with the evolution of kinetic energy, cohesive samples experience a delay in the migration and stabilisation, compared to the cohesionless samples. Hence, this signifies a less brittle response when cohesion is included.

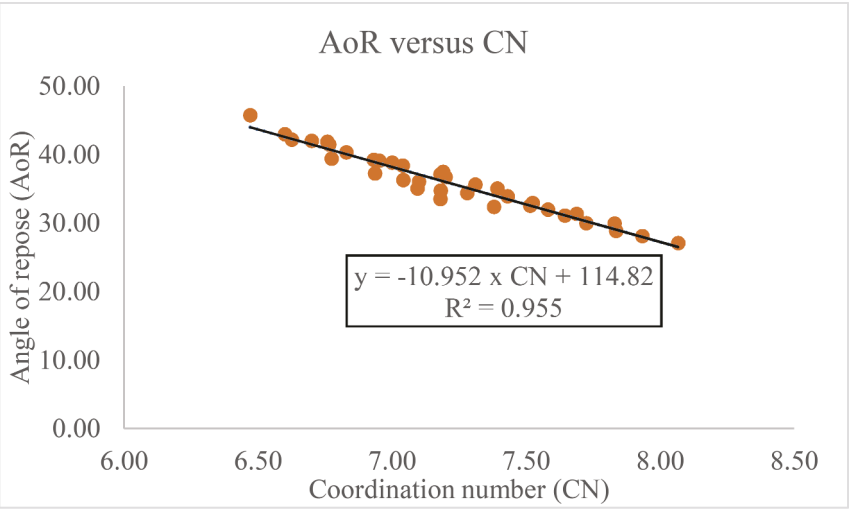

Figure 12. Quantitative relationships between AoR and CN for varying cohesion and rolling friction levels.

3.4 *Linkage between macro-parameters and micro-parameters*

The current study has revealed that both the angle of repose (AoR) and the micro-scale coordination number (CN) are directly affected by the particle-scale parameters such as the cohesion and friction effects. With the data available, this study attempts to propose a linkage between the macro-parameter AoR and the micro-parameter CN for materials for all cohesion and rolling friction levels. The correlations between the AoR and CN values are depicted very well by the fitted regression lines, with an error rate below 5% as shown in Figure 12. Moreover, the proposed equation demonstrates an inverse relationship between AoR and CN, which means a higher CN leads to a lower AoR, indicating increased stability of the slopes. In fact, a higher CN implies that the particles are more densely packed and have more contacts with their neighbours, resulting in a more stable structure. This stability is then reflected in a lower angle of repose. This explanation is also applied in the case of increasing cohesive and frictional forces, the system becomes looser (i.e., smaller CN) and the angle of repose can reach a higher slope without sliding (i.e., higher AoR).

3.5 *The cohesive effect on the strength-deformation behaviour in DST shear test*

Figure 13 shows the evolution of shear stress as observed in DEM simulations during shear tests on cohesionless (CED = 0) and cohesive state of soils with varying levels of cohesion. Compared to the non-cohesive dry sand samples, cohesive effects contribute to an enhanced shear strength, which becomes more pronounced with increasing cohesion levels. For example, when the cohesion energy density CED is low (i.e., CED < 5 x 10^5), the stress-strain curve in the simulations experiences a slight upward shift, reflecting the higher peak shear stresses and residual stresses, which is quite similar with the behaviour of wet samples with 10 % water content from experiments. However, this shift is minimal as the capillary forces, also known as the weak apparent cohesion, have a limited effect on soil strength under external loading.

Figure 13 also shows the dilation characteristics influenced by the cohesive effects in soils in the direct shear test. The results indicate that when cohesive forces increase, the samples displace more substantially in the vertical direction. The reason for this effect is that the addition of cohesion causes particles to behave as agglomerates or clumps, resulting in a larger dilation angle and

a higher friction angle. In order words, with the addition of cohesion, agglomerated particles are mobilised by a larger force and hence, the soil exhibits a greater resistance to shearing.

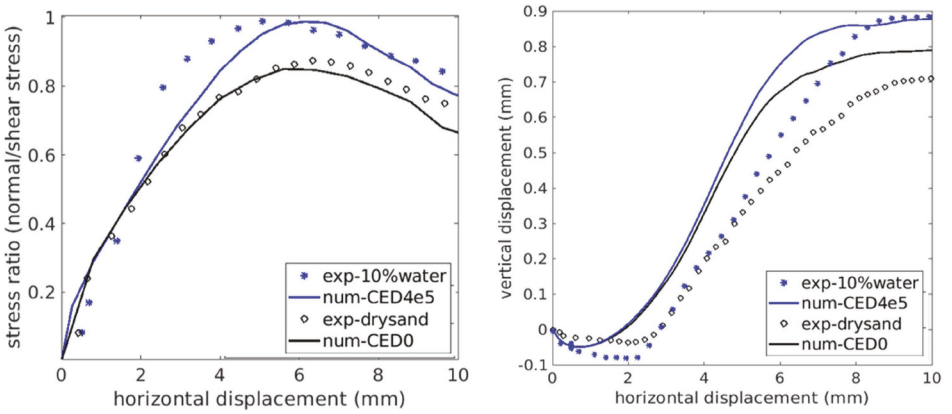

Figure 13. The development of shear stress and vertical movement under varying cohesion levels in DEM a) shear stress versus horizontal displacement at a normal stress 45 kPa, b) vertical displacement versus horizontal displacement.

4 CURRENT CHALLENGES AND FUTURE STUDIES

Although significant efforts have gone to modelling particle contacts in the past years, yet the current state of DEM contact models, especially considering cohesive behaviour still remains considerable challenges that prevent predictions from higher accuracy. Some of them can be pointed out, thus suggestions for future studies as follows:

1. As the generic formulation of the JKR contact radius is mathematically challenging, the simplified JKR (SJKR) model takes on a circular form as proposed in Hertzian theory. More computational efforts are needed to solve the equation of the real contact radius in cohesive contact model, so that more accurate load-deformation behaviour of various materials can be simulated.
2. The cohesion forces provided by JKR model will diminish when the normal deformation δ_n reaches negative values, therefore, this model is applicable to model the short-range attraction forces between particles, whereas the separation distance is minimal, rather than the long-range attraction forces.
3. The current JKR model was developed to extend the Hertz theory to capture the elaso-cohesive contacts, while solutions for modelling visco-elastic and plastic effects are still incomplete. As visco- and elasto-plastic behaviours often exhibit in soils, significant efforts are required to develop more detailed and realistic contact models for DEM simulations.

5 CONCLUSIONS AND PRACTICAL IMPLICATIONS

Advanced numerical DEM studies were conducted to investigate the mechanism and the influences of micro-scale cohesive contacts on the macro-behaviour of soils. Varying degrees of cohesion between particles were incorporated to study the cohesive behaviour of soils under different conditions such as the free-flow and shear. Critical findings of this study can be collated as follows:

1) The cohesive behaviour of soils, despite its significant influence on the stability of soils, remained considerable ambiguity in terms of its microscale mechanism and effects. The current extensive investigation using DEM study to examine the cohesive effect of material found out that when the cohesive effect was ignored, it can lead to the underestimation of the angle of repose. In fact, the AoR value was reported as a function of the micro-scale cohesion since the higher the cohesive forces, the higher AoR values.

2) The results also revealed that increasing cohesion levels led to a higher apparent porosity regardless of the level of friction. Such a response of increasing porosity can be attributed to the tendency to form chain-connected structures, as well as large agglomerates among cohesive particles.
3) The empirical relationships ($R^2 > 0.98$) between the macro-scale AoR and micro-scale coordination number CN were established for the first time considering different levels of cohesion. The equations demonstrated the inverse relationship between AoR and CN, meaning that a higher CN signified a smaller AoR value. As when CN increased, the gravity-induced densification process was enhanced significantly and particles were more vulnerable to moving, leading to a smaller AoR value.
4) This study also demonstrated that not only the interparticle cohesive effects were dominant in the free-flowing condition, but also they can significantly alter shear behaviour of soil under loading. When cohesion was present, the shear strength of the cohesive samples was significantly higher than that in cohesionless state, and this feature was expected to become more pronounced with increasing cohesion levels.
5) Moreover, with the presence of cohesive forces, the samples experienced a greater degree of expansion in the vertical direction (i.e., dilation) than the cohesionless samples. This is because the addition of interparticle cohesion linked particles into agglomerates through increased particle connections and bridging, which were mobilised by a larger dilation angle and friction angle.
6) The practical implication of this study is to promote a better understanding of the micro-cohesive effect on soil behaviour and to use this understanding in geotechnical designs and analysis. For instance, the strengthening effect of the interparticle cohesion on the shear strength of materials can provide significant values to ground improvement in practical applications if they are appropriately combined with frictional components.

ACKNOWLEDGEMENT

This research was supported by Transport Research Centre (TRC, UTS), and the Australian Government through the Australian Research Council's Linkage Projects funding scheme (project **LP160101254**). Technical and financial support from industry partners including SMEC, Sydney Trains, ACRI and Coffey are greatly appreciated. Moreover, the contents of this paper include some critical outcomes that have been published previously. They have been cited where warranted, and the copyright clearance from the original sources has been granted to the authors to reproduce with kind permission.

REFERENCES

Ai, J., Chen, J.-F., Rotter, J. & Ooi, J. 2011. Assessment of rolling resistance models in discrete element simulations. *Powder Technology*, 206, 269–282.

Barthel, E. 2008. Adhesive elastic contacts: JKR and more. *Journal of Physics D: Applied Physics*, 41, 163001.

Beakawi Al-Hashemi, H. M. & Baghabra Al-Amoudi, O. S. 2018. A review on the angle of repose of granular materials. *Powder Technology*, 330, 397–417, https://www.sciencedirect.com/science/article/pii/S0032591018301153

Behjani, M. A., Rahmanian, N., Fardina Bt Abdul Ghani, N. & Hassanpour, A. 2017. An investigation on process of seeded granulation in a continuous drum granulator using DEM. *Advanced Powder Technology*, 28, 2456–2464, https://www.sciencedirect.com/science/article/pii/S0921883117300730

Cui, L. & O'sullivan, C. 2006. Exploring the macro- and micro-scale response of an idealised granular material in the direct shear apparatus. *Géotechnique*, 56, 455–468, https://doi.org/10.1680/geot.2006.56.7.455

Deng, X. L. & Davé, R. N. 2013. Dynamic simulation of particle packing influenced by size, aspect ratio and surface energy. *Granular Matter*, 15, 401–415, https://doi.org/10.1007/s10035-013-0413-0

Derakhshani, S. M., Schott, D. L. & Lodewijks, G. 2015. Micro–macro properties of quartz sand: Experimental investigation and DEM simulation. *Powder Technology*, 269, 127–138, https://www.sciencedirect.com/science/article/pii/S0032591014007888

Doan, T., Indraratna, B., Nguyen, T. T. & Rujikiatkamjorn, C. 2023. Interactive Role of Rolling Friction and Cohesion on the Angle of Repose through a Microscale Assessment. *International Journal of Geomechanics*, 23, 04022250, https://doi.org/10.1061/(ASCE)GM.1943-5622.0002632

Endres, S. C., Ciacchi, L. C. & Mädler, L. 2021. A review of contact force models between nanoparticles in agglomerates, aggregates, and films. *Journal of Aerosol Science*, 153, 105719, https://www.sciencedirect.com/science/article/pii/S0021850220302044

Goudarzy, M., Sarkar, D., Lieske, W. & Wichtmann, T. 2021. Influence of plastic fines content on the liquefaction susceptibility of sands: monotonic loading. *Acta Geotechnica*, https://doi.org/10.1007/s11440-021-01283-w

Gratchev, I. B., Sassa, K., Osipov, V. I. & Sokolov, V. N. 2006. The liquefaction of clayey soils under cyclic loading. *Engineering Geology*, 86, 70–84, https://www.sciencedirect.com/science/article/pii/S0013795206001499

Hassanzadeh, V., Wensrich, C. M. & Moreno-Atanasio, R. 2020. Elucidation of the role of cohesion in the macroscopic behaviour of coarse particulate systems using DEM. *Powder Technology*, 361, 374–388, https://www.sciencedirect.com/science/article/pii/S0032591019305625

Jones, R. 2003. From Single Particle AFM Studies of Adhesion and Friction to Bulk Flow: Forging the Links. *Granular Matter*, 4, 191–204, https://doi.org/10.1007/s10035-002-0122-6

Li, Y., Xu, Y. & Thornton, C. 2005. A comparison of discrete element simulations and experiments for 'sandpiles' composed of spherical particles. *Powder Technology*, 160, 219–228, https://www.sciencedirect.com/science/article/pii/S0032591005004079

Lommen, S., Schott, D. & Lodewijks, G. 2014. DEM speedup: Stiffness effects on behavior of bulk material. *Particuology*, 12, 107–112, https://www.sciencedirect.com/science/article/pii/S1674200113001387

Mason, T., Levine, A., Ertaş, D. & Halsey, T. T. C. 1999. Critical angle of wet sandpiles. *Physical review. E, Statistical physics, plasmas, fluids, and related interdisciplinary topics*, 60, R5044–7.

Mitarai, N. & Nori, F. 2006. Wet granular materials. *Advances in Physics*, 55, 1–45, https://doi.org/10.1080/00018730600626065

Mitchell, J. K. & Soga, K. 2005. *Fundamentals of soil behavior*, John Wiley & Sons New York.

Nguyen, T. T. & Indraratna, B. 2020a. A Coupled CFD–DEM Approach to Examine the Hydraulic Critical State of Soil under Increasing Hydraulic Gradient. *International Journal of Geomechanics*, 20, 04020138, https://doi.org/10.1061/(ASCE)GM.1943-5622.0001782

Nguyen, T. T. & Indraratna, B. 2020b. The energy transformation of internal erosion based on fluid-particle coupling. *Computers and Geotechnics*, 121, 103475, https://www.sciencedirect.com/science/article/pii/S0266352X20300380

Ni, Q., Powrie, W., Zhang, X. & Harkness, R. 2000. Effect of Particle Properties on Soil Behavior: 3-D Numerical Modeling of Shearbox Tests. *Numerical Methods in Geotechnical Engineering*.

O'sullivan, C. 2011. *Particulate discrete element modelling a geomechanics perspective*, London, Taylor & Francis.

Parteli, E. J. R., Schmidt, J., Blümel, C., Wirth, K.-E., Peukert, W. & Pöschel, T. 2014. Attractive particle interaction forces and packing density of fine glass powders. *Scientific Reports*, 4, 6227. https://doi.org/10.1038/srep06227

Phan, Q. T., Bui, H. H., Nguyen, G. D. & Bouazza, A. 2021. Effect of particle rolling resistance on drained and undrained behaviour of silty sand. *Acta Geotechnica*, 16, 2657–2682, https://doi.org/10.1007/s11440-020-01128-y

Roessler, T. & Katterfeld, A. 2019. DEM parameter calibration of cohesive bulk materials using a simple angle of repose test. *Particuology*, 45, 105–115, https://www.sciencedirect.com/science/article/pii/S1674200119300033

Rognon, P., Roux, J.-N., Wolf, D., Naaim, M. & Chevoir, F. 2007. Rheophysics of cohesive granular materials. *EPL (Europhysics Letters)*, 74, 644.

Terzaghi, K. 1943. *Theoretical Soil Mechanics*, Wiley, New York.

Wang, J.-P., Li, X. & Yu, H.-S. 2018. A micro–macro investigation of the capillary strengthening effect in wet granular materials. *Acta Geotechnica*, 13, 513–533, https://doi.org/10.1007/s11440-017-0619-0

Xu, J. Q., Zou, R. P. & Yu, A. B. 2007. Analysis of the packing structure of wet spheres by Voronoi–Delaunay tessellation. *Granular Matter*, 9, 455–463, https://doi.org/10.1007/s10035-007-0052-4

Yu, A., Liu, L., Zhang, Z., Yang, R. & Zou, R. 2003. Computer simulation of the packing of particles. *International Journal of Materials & Product Technology - INT J MATER PROD TECHNOL*, 19

Zhu, H. P., Zhou, Z. Y., Yang, R. Y. & Yu, A. B. 2007. Discrete particle simulation of particulate systems: Theoretical developments. *Chemical Engineering Science*, 62, 3378–3396, https://www.sciencedirect.com/science/article/pii/S000925090700262X